Available online at www.sciencedirect.com
SCIENCE DIRECT
International Journal of Mass Spectrometry 249–250 (2006) 93–105
International Journal of Mass Spectrometry
www.elsevier.com/locate/ijms

# Fragmentation of doubly-protonated peptide ion populations labeled by H/D exchange with $CD_3OD$

Kristin A. Herrmann [1], Krishna Kuppannan [2], Vicki H. Wysocki *

*University of Arizona, Department of Chemistry, 1306 E. University Blvd., Tucson, AZ 85721-0041, USA*

Received 7 November 2005; received in revised form 22 December 2005; accepted 27 December 2005
Available online 14 February 2006

**Abstract**

Doubly-protonated bradykinin (RPPGFSPFR) and an angiotensin III analogue (RVYIFPF) were subjected to hydrogen/deuterium (H/D) exchange with $CD_3OD$ in a Fourier transform ion cyclotron resonance (FT-ICR) mass spectrometer. A bimodal distribution of deuterium incorporation was present for bradykinin after H/D exchange for 90 s at a $CD_3OD$ pressure of $4 \times 10^{-7}$ Torr, indicating the existence of at least two distinct populations. Bradykinin ion populations corresponding to 0–2 and 5–11 deuteriums (i.e., $D_0$, $D_1$, $D_2$, $D_5$, $D_6$, $D_7$, $D_8$, $D_9$, $D_{10}$, and $D_{11}$) were each monoisotopically selected and fragmented via sustained off-resonance irradiation (SORI) collision-induced dissociation (CID). The $D_0$–$D_2$ ion populations, which correspond to the slower exchanging population, consistently require lower SORI amplitude to achieve a similar precursor ion survival yield as the faster-reacting ($D_5$–$D_{11}$) populations. These results demonstrate that conformation/protonation motif has an effect on fragmentation efficiency for bradykinin. Also, the partitioning of the deuterium atoms into fragment ions suggests that the C-terminal arginine residue exchanges more rapidly than the N-terminal arginine. Total deuterium incorporation in the $b_1/y_8$ and $b_2/y_7$ ion pairs matches very closely the theoretical values for all ion populations studied, indicating that the ions of a complementary pair are likely formed during the same fragmentation event, or that no scrambling occurs upon SORI. Deuterium incorporation into the $y_1/a_8$ pseudo-ion pair does not closely match the expected theoretical values. The other peptide, doubly-protonated RVYIFPF, has a trimodal distribution of deuterium incorporation upon H/D exchange with $CD_3OD$ at a pressure of $1 \times 10^{-7}$ Torr for 600 s, indicating at least three distinct ion populations. After 90 s of H/D exchange where at least two distinct populations are detected, the $D_0$–$D_7$ ion populations were monoisotopically selected and fragmented via SORI-CID over a range of SORI amplitudes. The precursor ion survival yield as a function of SORI amplitude falls into two distinct behaviors corresponding to slower- and faster-reacting ion populations. The slower-reacting population requires larger SORI amplitudes to achieve the same precursor ion survival yield as the faster exchanging population. Total deuterium incorporation into the $y_2/b_5$ ion pairs matches closely the theoretical values over all ion populations and SORI amplitudes studied. This result indicates the $y_2$ and $b_5$ ions are likely formed by the same mechanism over the SORI amplitudes studied.


*Keywords:* H/D exchange; b- and y-fragment ions; Peptide conformation; Bradykinin; Angiotensin III analogue

## 1. Introduction

The investigation of the gas phase conformation of biologically relevant molecules such as proteins and peptides has been an area of recent interest because of the desire to understand the relationship between solution and anhydrous (i.e., gas phase) structures, and because gas phase structures are fragmented in analytical mass spectrometry experiments [1,2]. Investigating gas phase structure will aid in the understanding of the role solvation plays in solution phase protein and peptide structures [3]. The three-dimensional gas phase conformation of proteins and peptides is also important because unimolecular dissociation may be affected by the conformation and/or protonation motifs of the molecule [4–6]. Different conformations/protonation motifs sometimes have different fragmentation patterns, as recently demonstrated for an aspartic acid containing fixed charge derivative peptide [7]. Both ion mobility and hydrogen/deuterium (H/D) exchange have been used to investigate gas phase isomers [8–11]. Ion mobility relies on different collisional cross-sections to separate different conformers, while H/D exchange relies on a difference in the rate of exchange with a deuterated reagent.

* Corresponding author. Tel.: +1 520 621 2628; fax: +1 520 621 8407.
*E-mail address:* vwysocki@u.arizona.edu (V.H. Wysocki).
[1] Present address: Tate & Lyle, 2200 E. Eldorado St., Decatur, IL 62525, USA.
[2] Present address: The Dow Chemical Company, Analytical Sciences, 1897 Building, Midland, MI 48667, USA.

1387-3806/$ – see front matter © 2006 Elsevier B.V. All rights reserved.
doi:10.1016/j.ijms.2005.12.047

Presumably, hydrogen atoms which are strongly involved in hydrogen bonding or which are not accessible on the surface of the peptide will not readily exchange for deuterium. Gas phase H/D exchange reactions are commonly studied in a Fourier transform ion cyclotron resonance (FT-ICR) mass spectrometer at a reagent pressure of $10^{-7}$–$10^{-5}$ Torr and for times up to several minutes or hours [10,12,13]. The most common exchange reagents are $ND_3$, $CD_3OD$, and $D_2O$. Of the reagents listed here, exchange reactions with $ND_3$ are the most facile and are thought to occur through an onium ion or tautomer mechanism [13]. $D_2O$ is generally the slowest reagent and exchange occurs through the relay mechanism in which $D_2O$ inserts into a proton bridge between two heteroatoms, or the flip-flop mechanism (for carboxylic acid functional groups) [13,14]. The onium ion mechanism is unlikely with $D_2O$ given its low gas phase basicity. Exchange reactions with $CD_3OD$ are also thought to occur through the relay mechanism, or the flip-flop mechanism for carboxylic acid functional groups.

The ion mobility and H/D exchange of the nonapeptide bradykinin and related analogues have been extensively studied [10,12,15–28]. Ion mobility measurements have shown that the singly- and doubly-protonated ions of bradykinin have a similar cross-section, while the triply-protonated ion has a cross-section that is approximately 15% larger, providing evidence for a much less compact structure [15–17]. H/D exchange studies with $D_2O$, $CD_3OD$, $ND_3$, and DI have detected two non-interconverting ion populations for doubly- and triply-protonated bradykinin [20,22,24–27]. These ion populations were not detected by traditional ion mobility experiments [15–17], suggesting the conformers have a similar collisional cross-section. Another possibility is that the conformations are different in the two instruments because of different timescales (milliseconds in ion mobility and minutes in FT-ICR). The bradykinin ions may be folding or unfolding on the longer timescale of the FT-ICR during accumulation in the hexapole or during the H/D exchange experiment. Calculation of site-specific rate constants by Lifshitz and co-workers revealed the first three exchanges of doubly-protonated bradykinin with $CD_3OD$ and $ND_3$ have equivalent rate constants [24]. They attribute these first three exchanges to the hydrogens at the protonated amino terminus. Later studies by Guevremont and co-workers using high-field asymmetric waveform ion mobility spectrometry (FAIMS) combined with H/D exchange detected four separate bradykinin populations, including one of very low abundance, for the doubly-protonated peptide [23]. In general, ion mobility and H/D exchange results support a compact, folded conformation for both singly- and doubly-protonated bradykinin in which the basic and acidic sites interact [10,16,29]. The existence of a salt-bridge, in which the carboxy terminus is deprotonated and both arginine residues are protonated, has been proposed for singly- and doubly-protonated bradykinin [27,28]. In doubly-protonated bradykinin, the amino terminus, which is the third most basic site on the peptide, is also likely protonated in the inactivated salt-bridge structure.

Fragmentation studies of bradykinin have also been reported. In slow-heating ion activation methods, peptides tend to fragment at the amide bond, resulting in the formation of $b_n$ and $y_n$ ions, where $n$ is the number of amino acid residues counting from the N- or C-terminus, respectively [30]. The fragmentation of doubly-protonated peptides often results in the formation of $b_n/y_{m-n}$ ion pairs, in which each ion is singly-protonated and $m$ is the total number of amino acid residues in the peptide. Presumably, these ion pairs can be formed simultaneously by the same mechanism if, when the amide bond cleaves, one ionizing proton is located on each of the newly formed $b_n$ and $y_{m-n}$ ions. Williams and co-workers have shown by blackbody infrared dissociation (BIRD) that the lowest energy fragmentation pathway for doubly-protonated bradykinin results in the formation of the $b_2/y_7$ ion pair [29]. This is supported by molecular dynamics simulations which demonstrate the protonated N-terminal arginine is partially solvated by the backbone carbonyl oxygen of the proline residue in the second position, which likely contributes to formation of the $b_2$ and $y_7$ ions [29].

Attempts to combine ion-molecule reactions with fragmentation studies of bradykinin have been reported. McLuckey and co-workers observed two ion populations for doubly-protonated bradykinin with different rates of hydroiodic acid attachment in an approximate ratio of 55:45 (for slow- and fast-reacting populations) [26]. Upon isolation and fragmentation of the slow-reacting ion population, they observed a mass spectrum identical to the mixture of populations, indicating interconversion of the ion populations. Also, the slower-reacting population could be converted back to the mixture of conformations through gentle activation [26]. Lifshitz and co-workers attempted to fragment doubly-protonated bradykinin labeled via H/D exchange with $ND_3$ [24]. They observed a shift of three mass units for the $y_6$ and $y_7$ ions, and two mass units for the $b_6$ ion. Also, they report the neutral loss of water from the precursor ion does not contain any deuterium [24]. However, they also report any conclusions based on these data are tentative because the ionizing proton at the amino terminus is expected to be mobile (assuming a salt-bridge structure), thereby causing deuterium scrambling upon ion activation [24]. In fact, scrambling of "mobile" protons and deuteriums in peptides is well-documented in the literature [31–34]. Mao and Douglas performed H/D exchange of bradykinin fragment ions $y_6$, $y_7$, $y_8$, $y_8^{2+}$, $b_5$, $a_6$, $b_6$, and $a_8$ and observed that the y-ions exchange more readily [22]. They conclude this is consistent with the higher exchange level observed for singly-protonated des-arg$^1$-bradykinin over singly-protonated des-arg$^9$-bradykinin [22].

Here, the SORI-CID fragmentation of ion populations separated by H/D exchange of doubly-protonated bradykinin with $CD_3OD$ is reported. These populations may differ in the spatial distribution of the atoms (i.e., conformation) or in the location of the protons and hydrogen-bonding scheme (i.e., the protonation motif). In addition, upon ion activation, ion populations may convert into other conformations/protonation motifs. The FT-ICR allows monoisotopic selection of both the precursor ion and individual ion populations following the labeling experiment. These experiments reveal some differences in the energetics of fragmentation for different ion populations. Also, the deuterium content of fragment ions and $b_n/y_{m-n}$ ion pairs is examined. In addition to the studies presented here for doubly-protonated bradykinin, the fragmentation of ion populations labeled by H/D

exchange for the doubly-protonated peptide RVYIFPF is also reported. RVYIFPF is an analogue of angiotensin III in which the histidine residue in the fifth position has been replaced with phenylalanine. This peptide is of interest because, upon H/D exchange of the doubly-protonated species, distinct ion populations are detected. Differences in the fragmentation of ion populations and the partitioning of deuterium atoms into a $b_n/y_{m-n}$ ion pair are discussed.

## 2. Experimental

### 2.1. Materials

The angiotensin III peptide analogue RVYIFPF (where R is arginine, V valine, Y tyrosine, I isoleucine, F phenylalanine, and P is proline) was prepared using solid phase synthesis protocols reported previously [35]. 9-Fluoroenylmethoxy-carbonyl (Fmoc) derivatives of the amino acids were purchased from Advanced Chemtech (Louisville, KY). The first residue (C-terminal residue of the finished peptide) was purchased bound to the Wang resin, from Calbiochem/Novabiochem (San Diego, CA). $CD_3OD$ (99.9%) was purchased from Cambridge Isotope Laboratories (Andover, MA) and degassed through several freeze–thaw cycles before use. $CH_3OH$ (99.9%) used for D/H back-exchange reactions was purchased from Sigma–Aldrich (St. Louis, MO) and also degassed before use. Bradykinin (RPPGFSPFR, where G is glycine and S is serine) and all other reagents required were purchased from Sigma–Aldrich and used without further purification.

### 2.2. FT-ICR H/D exchange and fragmentation

Ions were generated using an Analytica (Branford, CT) second generation electrospray (ESI) source. An IonSpec (Lake Forest, CA) 4.7 T Fourier transform ion cyclotron resonance (FT-ICR) instrument was used for H/D exchange and fragmentation studies. A pulsed-leak configuration described by Freiser and co-workers [36] was incorporated to allow a constant reagent gas pressure in the analyzer region for the desired exchange time.

The ions were introduced into the instrument by infusing 10–30 μM solutions of the peptides in 50:50 methanol:water with 1% acetic acid using a stainless steel microelectrospray needle (0.004″ i.d.) at a flow rate of 2–3 μL/min. For the D/H back-exchange experiment (i.e., labeling in solution and gas phase D/H back-exchange with $CH_3OH$), the bradykinin solution was prepared 1 h before analysis with 50:50 $CD_3OD$:$D_2O$ and 1% undeuterated acetic acid. The source temperature was 180–200 °C, and 3.8 kV was applied to the electrospray needle. The instrument has two regions of differential cryogenic pumping, referred to as the source and analyzer regions, with a typical analyzer base pressure of $7 \times 10^{-11}$ Torr. The electrosprayed ions pass through a skimmer, and are collected in an external rf-only hexapole, where they are allowed to accumulate for 300–1000 ms before being passed into the analyzer through a shutter. An rf-only quadrupole guides the ions into the cylindrical ICR cell. Once the ions were trapped inside the ICR cell, the precursor ion was monoisotopically isolated by ejecting all other mass-to-charge values with a frequency sweep. Ions were allowed to exchange with constant $CD_3OD$ pressure. Heating of the ions occurs upon monoisotopic selection, causing some fragmentation when the reagent gas is leaked into the ICR cell. It is assumed the remaining precursor ions are collisionally cooled after several seconds of interaction with $CD_3OD$. After the appropriate exchange time, a 40 s pump-down time was applied to remove neutral reagents and achieve the low pressures necessary for FT-ICR analysis. During this pump-down time, isolation of individual ion populations and sustained off-resonance irradiation (SORI) collision-induced dissociation (CID) fragmentation was sometimes performed, as described below. H/D exchange of the fragment ions is negligible since the pressure in the ICR cell has dropped to approximately $5 \times 10^{-9}$ Torr before fragmentation of the precursor ion. One to 30 transients were averaged depending on the strength of the ICR signal.

All H/D exchange reactions with doubly-protonated bradykinin were carried out with a $CD_3OD$ pressure of $4 \times 10^{-7}$ Torr. In order to examine the fragmentation of ion populations with 5–11 deuteriums incorporated, the precursor ion ($m/z$ 530.8) was first monoisotopically selected and exposed to the $CD_3OD$ reagent for 90 s. Following H/D exchange, the ion populations corresponding to 5–11 deuteriums were each monoisotopically selected and fragmented via SORI-CID with argon as the collision gas. The monoisotopic isolation window and amplitude of the pulse ejecting other ions was kept consistent for each ion population. SORI time was 500 ms and SORI amplitude was 3 V. Pressure in the ICR cell at the time of detection was approximately $2 \times 10^{-9}$ Torr.

The relative abundance of the doubly-protonated bradykinin ion populations corresponding to zero to two deuteriums incorporated after 90 s exchange was too low to perform both monoisotopic selection of the precursor ion and the individual ion population. Therefore, *non-monoisotopic* isolation of the precursor ion was performed. After 90 s exchange, the ion populations corresponding to zero to two deuteriums incorporated were monoisotopically selected and fragmented via SORI-CID as described above for the ion populations with 5–11 deuteriums incorporated. In addition to performing a 3 V SORI-CID experiment for ion populations with zero to two deuteriums incorporated, a 2.75 V SORI-CID experiment was also performed to ensure the selected ion population was fragmented to approximately the same survival yield (i.e., within 5%) as the $D_5$–$D_{11}$ populations. Since non-monoisotopic isolation of the precursor ion was not performed for the population with one deuterium incorporated, the isotopic distribution of the fragmentation peaks was deconvoluted. This was accomplished by taking into account the natural isotopic abundance of the precursor ion and the statistical probability of a $^{13}C$ atom being located in each fragmentation ion. Deconvolution of the ion population with two deuteriums incorporated was not attempted.

D/H back-exchange reactions with solution labeled doubly-charged bradykinin were carried out with a $CH_3OH$ pressure of $6 \times 10^{-7}$ Torr. SORI-CID was also performed after D/H back-exchange. In this experiment, the labeled doubly-protonated precursor ion was reacted with the $CH_3OH$ reagent gas for

90 s. Monoisotopic selection was not performed because H/D exchange of the peptide was performed in solution prior to gas phase D/H back-exchange. Following D/H back-exchange, the envelope of peaks corresponding to the "slow" and "fast" exchanging populations were each isolated and fragmented with a 500 ms, 2.75 V or 3 V SORI pulse with argon as the collision gas.

All FT-ICR H/D exchange reactions with $[RVYIFPF + 2H^{2+}]$ were carried out with a $CD_3OD$ pressure of $1 \times 10^{-7}$ Torr. In order to monitor the amount of exchange as a function of time, the precursor ion (*m/z* 471.3) was monoisotopically selected and subjected to H/D exchange for 0–600 s. Pressure in the ICR at the time of detection was approximately $1 \times 10^{-9}$ Torr. The first apparent rate constant was calculated by assuming pseudo-first order kinetics because the exchange reagent is considered to be in great excess of the analyte. Although the instrument was not pre-conditioned with the deuterating agent, isotopic purity was measured with betaine, a compound with one exchangeable hydrogen and a known rate constant [13]. The exchange of betaine with $CD_3OD$ was >90% complete, and so contamination and back-exchange was considered negligible. Subsequent apparent rate constants were estimated by the peaks in the exchange time plots where product formation and depletion rates are equivalent [13]. Exchange reagent pressure was corrected for ion gauge sensitivity for the water reagent [37] and the ion gauge (Granville-Phillips, Bayard-Alpert type) was calibrated using the H/D exchange reaction of betaine [13].

$[RVYIFPF + 2H]^{2+}$ ion populations labeled by H/D exchange were monoisotopically selected and fragmented. The precursor ion was first monoisotopically selected and exposed to the $CD_3OD$ reagent (pressure = $1 \times 10^{-7}$ Torr) for 60 s. Following this 60 s H/D exchange, the ions corresponding to zero to seven deuteriums were each monoisotopically isolated and fragmented via SORI-CID. The monoisotopic isolation window and amplitude of the pulse ejecting other ions was kept consistent for each ion population. SORI time was 500 ms while SORI amplitude was varied from 0 to 1.5 V. Fragmentation is observed when SORI amplitude is set to 0 V and collision gas is introduced due to heating of the ions during the isolation step. Argon was used as the collision gas and the 500 ms gas pulse started with the beginning of the SORI pulse. Pressure in the ICR at the time of detection was approximately $1 \times 10^{-9}$ Torr. In a separate experiment, $[RVYIFPF + 2H]^{2+}$ was monoisotopically selected and reacted with $CD_3OD$ (pressure = $1 \times 10^{-6}$ Torr) for 60 s. Following the H/D exchange step, the envelopes of peaks corresponding to $D_0 - D_5$ and $D_6 - D_{12}$ were isolated and fragmented over a range of SORI amplitudes (0–3 V).

### 2.3. Ion trap H/D exchange

$[RVYIFPF + 2H]^{2+}$ was subjected to H/D exchange with $D_2O$ in a ThermoFinnigan ESI-quadrupole ion trap (QIT). H/D exchange in the QIT is complementary to FT-ICR exchange because the QIT exchange reagent pressure is about four orders of magnitude greater, although exchange time is practically limited to less than 1 min. The instrument was modified to accommodate H/D exchange reactions as described by Gronert [38]. In this system, $D_2O$ is mixed with the helium flow gas and introduced into the instrument. The RVYIFPF peptide solution (approximately 50 μM) in 50:50 methanol:water with 1% acetic acid was infused into the instrument at a flow rate of 8 μL/min. The instrument was first conditioned with $D_2O$ for approximately 1 h to remove any hydrogen contamination. The $[RVYIFPF + 2H]^{2+}$ ion was isolated with a 10 mass-to-charge unit window and allowed to exchange for 10 s at a $D_2O$ reagent pressure of approximately $10^{-3}$ Torr.

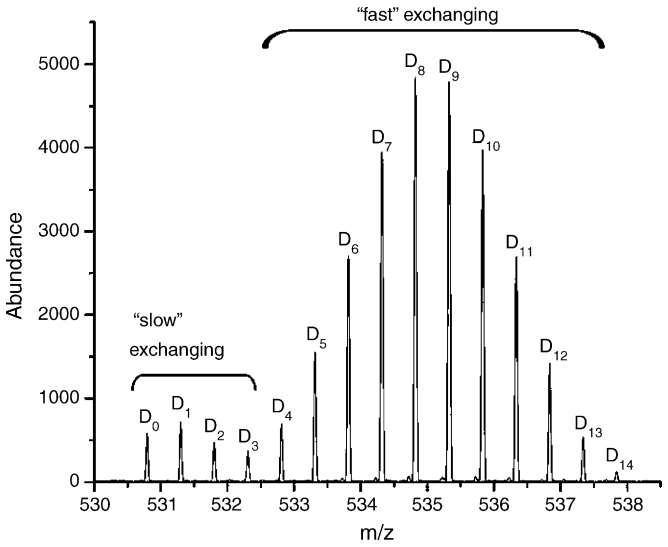


Fig. 1. Monoisotopic isolation and H/D exchange of $[RPPGFSPFR + 2H]^{2+}$ with $CD_3OD$ at $4 \times 10^{-7}$ Torr for 90 s. Peaks are labeled as $D_n$, where *n* indicates the number of hydrogens which have been exchanged for deuterium.

## 3. Results and discussion

### 3.1. H/D exchange of doubly-protonated bradykinin

The doubly-protonated, 9 amino acid residue peptide bradykinin $[RPPGFSPFR + 2H]^{2+}$ contains 19 labile hydrogens, including 1 carboxy terminus, 1 serine, 2 amino terminal, 5 backbone amide, and 8 arginine hydrogens, plus 2 ionizing protons. The monoisotopic isolation and H/D exchange of doubly-protonated bradykinin with $CD_3OD$ at a pressure of $4 \times 10^{-7}$ Torr for 90 s is shown in Fig. 1. The presence of two distinct populations with different rates of exchange is observed. The difference between these populations is likely due to a difference in the spatial distribution of the atoms (i.e., conformation) and/or in the location of the protons and hydrogen-bonding scheme. The most abundant ions for the slower and faster exchanging populations are $D_1$ and $D_8$, respectively. The maximum number of exchanges observed at this timescale and reagent pressure is 14. Although the H/D exchange of bradykinin with deuterated methanol has been previously reported, [12,20,22,24] the data are shown here to demonstrate the distribution of the labeled ion populations used in the fragmentation studies discussed below.

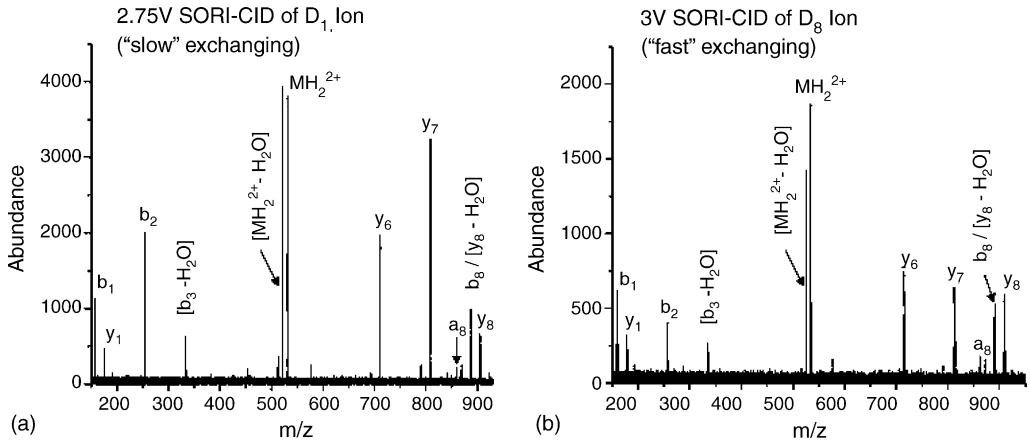


Fig. 2. SORI-CID spectra for: (a) monoisotopically selected $D_1$ population (precursor ion not monoisotopically selected before H/D exchange with $CD_3OD$ at $4 \times 10^{-7}$ Torr for 90 s), SORI time = 500 ms, amplitude = 2.75 V and (b) monoisotopically selected $D_8$ population (precursor ion monoisotopically selected before H/D exchange with $CD_3OD$ at $4 \times 10^{-7}$ Torr for 90 s), SORI time = 500 ms, SORI amplitude = 3.0 V.

### *3.2. Fragmentation of bradykinin ion populations labeled by H/D exchange*

Following monoisotopic isolation and H/D exchange of doubly-protonated bradykinin for 90 s at a $CD_3OD$ pressure of $4 \times 10^{-7}$ Torr, ion populations $D_5$, $D_6$, $D_7$, $D_8$, $D_9$, $D_{10}$, and $D_{11}$ were monoisotopically selected and fragmented via SORI-CID with argon as the collision gas. The same experiment was also performed for the $D_0$, $D_1$, and $D_2$ ion populations, except because of lower relative abundance, the precursor ion *before* H/D exchange was not monoisotopically selected. The SORI-CID spectra of the $D_1$ ($m/z$ 531.3) and $D_8$ ($m/z$ 534.8) ion populations are compared in Fig. 2. The amplitudes of the SORI pulses used to generate the spectra in Fig. 2 were chosen to deplete the abundance of the precursor ion to a similar value. SORI amplitudes of 2.75 V and 3 V SORI resulted in 11% and 14% survival yields of the isolated $D_1$ and $D_8$ precursor ions, respectively.

As shown in Fig. 2, fragmentation of the doubly-protonated precursor ion results in the formation of the ion pairs $b_1/y_8$ and $b_2/y_7$. An $a_8$ ion, which is presumably formed from the $b_8$ ion [39–43], is also observed. Because the $y_8$ ion and the $[b_8 + H_2O]$ ion coincidentally have the same elemental formula, the identity of the $y_8$ ion ($m/z$ = 904.5 in unlabeled peptide) was confirmed via MS/MS/MS ($MS^3$) experiments. The two main fragment ions observed upon SORI-CID fragmentation of the $m/z$ 904.5 ion (data not shown) are water loss and $y_6$, with no evidence of any b-type ions. Similarly, the $b_8$ and $[y_8 - H_2O]$ ions have the same elemental formula ($m/z$ = 886.5 in unlabeled peptide). The most abundant peak observed in the $MS^3$ fragmentation spectrum of $m/z$ 886.5 (data not shown) is $a_8$. However, y-type ions are also observed. Overall, b- and a-type ions are approximately three times as abundant as y-type ions when complete fragmentation of the $m/z$ 886.5 ion is performed ($a_8$ observed at 100% relative abundance; $b_2$, $[b_3 - H_2O]$, $y_1$, $y_3$, $y_4$, $[y_4 - H_2O]$, $y_5$, $[y_5 - H_2O]$, $y_6$, $[y_6 - H_2O]$ each observed at less than 20% relative abundance). Therefore, the ion observed at $m/z$ 886.5 (unlabeled peptide) in the MS/MS fragmentation of doubly-protonated bradykinin is labeled as a mixture of $b_8$ and $[y_8 - H_2O]$, but $b_8$ is the major component. Also observed in the fragmentation of doubly-protonated bradykinin is a large $y_6$ ion without the formation of the corresponding $b_3$ ion (Fig. 2). However, an ion observed at $m/z$ = 333.2 was found to have a measured exact mass of 333.2042, which agrees well with the theoretical exact mass of 333.2039 for $[b_3 - H_2O]$. In addition, fragmentation of $[MH_2^{2+} - H_2O]$ resulted in the formation of $y_6$ and $m/z$ 333.2. Although water cannot be lost from the side-chains of the first three amino acid residues (RPP), Ballard and Gaskell have shown that water loss can involve a backbone carbonyl [44].

The fragmentation of the "slow" and "fast" exchanging populations was studied as a function of SORI amplitude. The two populations were each selected as groups of ions, rather than monoisotopic isolation of individual peaks. Fig. 3 shows the precursor survival yield over a range of SORI amplitudes (2–4 V) for each population. The faster exchanging population

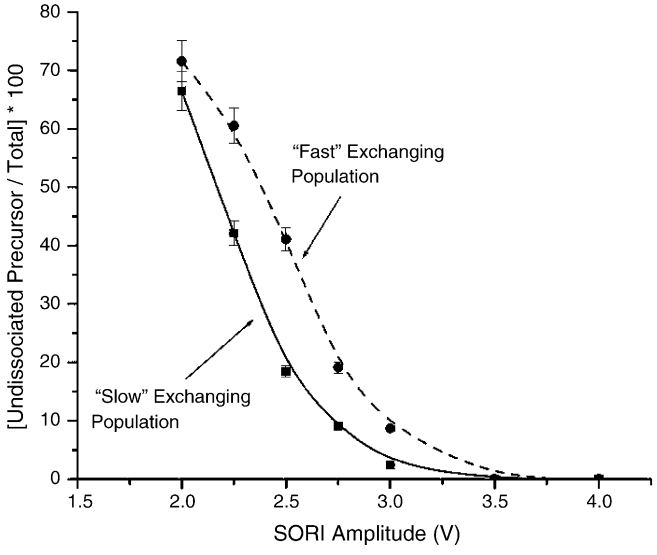


Fig. 3. Precursor survival yield for slower- and faster-exchanging bradykinin populations (H/D exchange with $CD_3OD$ at $4 \times 10^{-7}$ Torr for 90 s) as a function of SORI amplitude (SORI time = 500 ms).

consistently requires larger amplitude (approximately 0.25 V) to achieve similar precursor survival yields (within 5%) as the slower exchanging population. The conformational/protonation difference which attributes to the difference in fragmentation efficiency cannot be determined from these H/D exchange studies, but presumably the conformation, and its protonation/hydrogen bonding motif, is more favorable for fragmentation at lower energy in the "slower" exchanging population. Also, conversion of ion populations into other conformations/protonation motifs may occur during the activation event and thereby effect the observed spectrum. Another possibility is that the population more easily dissociated (slower-exchanging population) has a larger collisional cross-section, and therefore undergoes more collisions during a given excitation time SORI.

In order to determine if the difference in fragmentation efficiency of the "slow" (i.e., $D_0$–$D_2$) and "fast" (i.e., $D_5$–$D_{11}$) exchanging ion populations is due to a deuterium isotope effect, the peptide was subjected to solution phase H/D exchange. The labeled peptide was then reacted with $CH_3OH$ in the gas phase (i.e., D/H back-exchange). Fig. 4a shows the mass spectrum of the labeled peptide. Because the H/D exchange was carried out in solution, monoisotopic isolation was not possible. The peptide contains 19 labile hydrogens and, as shown in Fig. 4a, the majority of the ion population has exchanged the maximum number of hydrogens (inset in Fig. 4a shows isotopically corrected spectrum). The labeled peptide was back-exchanged in the gas phase with $CH_3OH$ at a pressure of $6 \times 10^{-7}$ Torr for 90 s, and the results are shown in Fig. 4b. As expected, two ion populations are observed, with the "faster" exchanging population more abundant. The envelope of peaks labeled in Fig. 4b as the "slow" exchanging population were isolated and fragmented via SORI-CID (SORI time = 500 ms, amplitude = 2.75 V), as shown in Fig. 4c. Similarly, the SORI-CID (SORI time = 500 ms, amplitude = 3 V) spectrum of the "fast" exchanging population is shown in Fig. 4d. The spectra shown in Fig. 4c and d are very similar to those in Fig. 2. Consistent with the H/D exchange experiment, the "slow" exchanging population, with a larger number of deuteriums, requires lower SORI amplitude than the "fast" exchanging population, with a smaller number of deuteriums, to achieve a similar precursor survival yield. Therefore, the difference in fragmentation efficiency between the two populations is observed regardless of which population contains more deuterium, and cannot be attributed to a deuterium isotope effect. Differences in fragmentation for different conformations/protonation motifs separated by gas phase exchange have been reported previously for a fixed-charge derivative peptide [7].

The overall picture that emerges from the results shown here is illustrated in Scheme 1a and b. Multiple conformations and/or structures for a given sequence exist in the gas

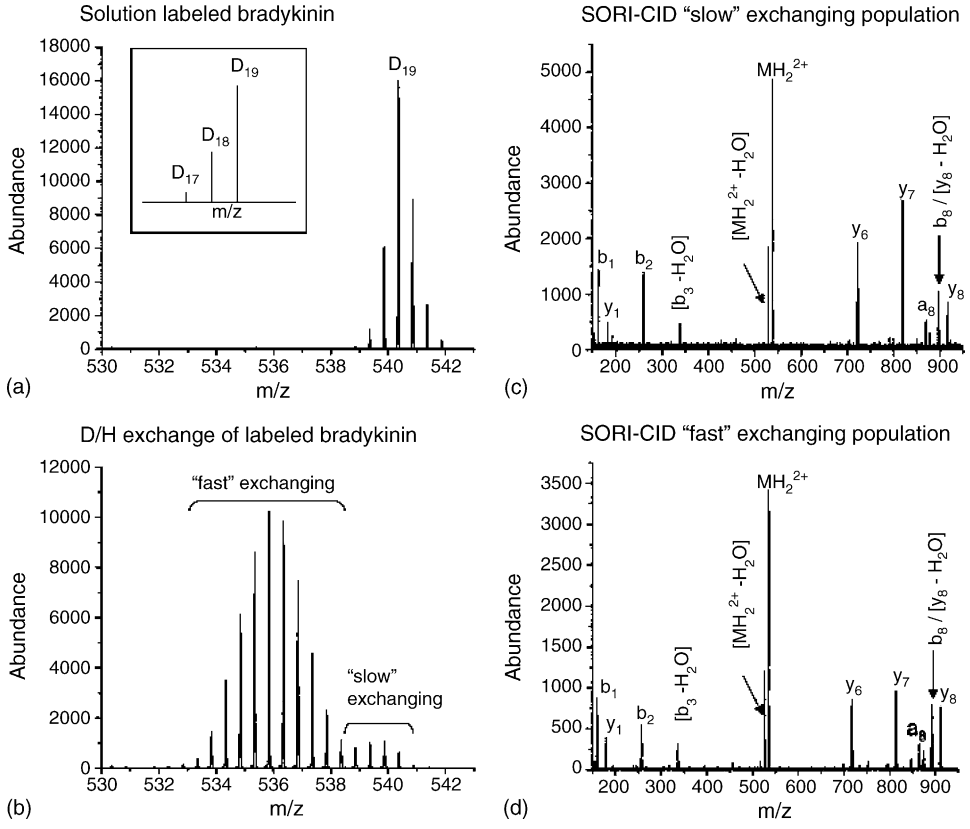


Fig. 4. (a) Mass spectrum of doubly-protonated bradykinin following incubation for 1 h in $D_2O$:$CD_3OD$:AcOH (50:50:2) solution, inset shows isotopically corrected spectrum; (b) D/H back-exchange of doubly-protonated bradykinin for 90 s (with $CH_3OH$ at a pressure of $6 \times 10^{-7}$ Torr) following incubation for 1 h in $D_2O$:$CD_3OD$:AcOH (50:50:2) solution, two populations are evident and labeled as "slow" and "fast"; (c) SORI-CID of "slow" exchanging doubly-protonated bradykinin population (SORI time = 500 ms, amplitude = 2.75 V); and (d) SORI-CID of "fast" exchanging doubly-protonated bradykinin population (SORI time = 500 ms, amplitude = 2.75 V). Compare with Figs. 1 and 2.

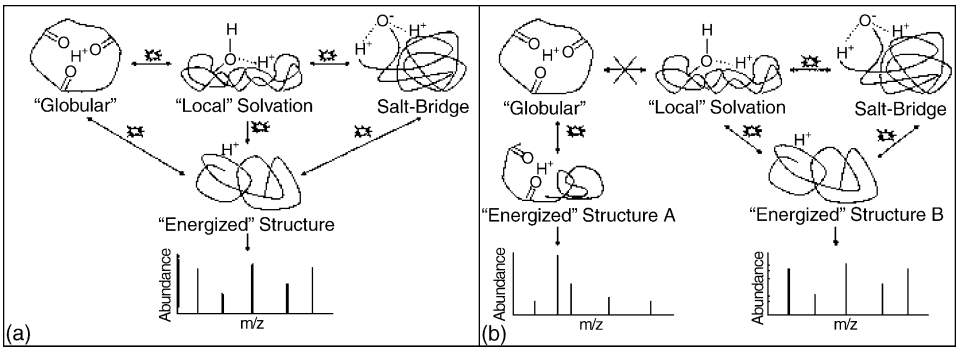


Scheme 1. (a) Generalized view of peptide fragmentation in which a common energized structure is formed upon ion activation. (b) Heterogeneous model of peptide fragmentation in which distinct energized structures are formed upon ion activation.

phase. Protonation schemes may include a globular structure in which the proton is heavily solvated by electronegative groups, a "local" solvation structure, or a salt-bridge structure (Scheme 1). These conformations/structures may have different reaction rates with the deuterating reagent, allowing them to be separated by H/D exchange and subsequently fragmentated. In the generalized view of peptide fragmentation (Scheme 1a), an "energized" structure is formed upon activation, and distinct populations no longer exist. The energized structure fragments, producing the observed mass spectrum. However, energy imparted to the ion during the activation step may not always convert distinct conformations/protonation motifs into one common structure. Instead, several distinct energized structures, depending on the structures before activation, may be formed as illustrated in Scheme 1b. In this "heterogeneous" model of peptide fragmentation, different energized structures may lead to different abundances and types of fragment ions, [7] or may have different fragmentation efficiencies, and the observed mass spectrum is a linear combination of these. Scheme 1b is a representative example of what may occur upon activation, although it is important to note that other protonation schemes may exist, and that the conversion of specific structures may be different (i.e., "local" solvation and salt-bridge structures may not necessarily lead to the same energized structure).

### 3.3. Partitioning of deuterium atoms after SORI-CID of the $D_8$ bradykinin ion population

As a representative example, the distribution of deuterium atoms in traditional- and pseudo-ion pairs following 500 ms, 3 V SORI-CID of the $D_8$ ion population is shown in Fig. 5. Fig. 5a and b shows the distribution of the deuterium atoms in the $b_1/y_8$ and $b_2/y_7$ ion pairs. The average number of deuteriums incorporated into the $b_1$ and $y_8$ ions is 2.5 and 5.5, respectively (Fig. 5a). The sum of the deuterium incorporation into the $b_1$ and $y_8$ ions from the $D_8$ precursor is 8.0, which matches the value of 8 expected if the deuteriums are partitioned between the two fragments. The $b_2/y_7$ ion pair (fragmentation between the two adjacent proline residues) is expected to partition the deuterium atoms identically to the $b_1/y_8$ ion pair (fragmentation between arginine and proline) since the amino acid residue proline contains no labile hydrogens. Indeed, the average number of deuteriums incorporated into the $b_2$ and $y_7$ ions is 2.5 and 5.5, respectively (Fig. 5b). The sum of the average deuterium incorporation is 8.0, again matching the total number of deuteriums of the selected precursor ion. If the fragment ions were formed by independent pathways and H/D scrambling occurred, the b and y fragments might contain unrelated numbers of deuterium that do not add up to the total amount of deuterium in the precursor. The close match to the theoretical values for $b_1/y_8$ and $b_2/y_7$ suggests these ion pairs truly are complementary, i.e., the ion pairs are likely formed simultaneously from the same fragmentation mechanism. If the $b_2$ and $y_7$ ions were formed by different mechanisms, there would be no expectation that the total number of deuteriums in the two mechanistically unrelated fragments would equal eight. If scrambling occurs either before or during the fragmentation event, it is not manifested in the partitioning of the deuterium atoms in a complementary pathway because both ions are formed *at the same time*.

Fig. 5c and d shows the partitioning of the deuterium atoms in the $y_1/b_8$ ion pair (with some contribution to $b_8$ from $[y_8 - H_2O]$, as discussed above) and the $[b_3 - H_2O]/y_6$ pseudo-ion pair after SORI-CID of the $D_8$ ion population. These results are discussed in further detail in the next section, along with the results from fragmentation of other ion populations.

### 3.4. Distribution of deuterium atoms after SORI-CID of the $D_1$–$D_2$ and $D_5$–$D_{11}$ bradykinin ion populations

The average number of deuterium atoms incorporated into each of the fragment ions observed is shown in Fig. 6a. As expected, the largest fragment ion, $[MH_2^{2+} - H_2O]$, retains the most deuterium. Upon fragmentation of the $D_{11}$ ion population, an average of 10 deuteriums are retained with the $[MH_2^{2+} - H_2O]$ fragment ion, and one is lost with the neutral water. Some amount of deuterium is lost with the neutral water for all populations studied. This disagrees with studies by Lifshitz and co-workers which reported no loss of deuterium with the neutral loss of water [24]. However, their H/D exchange step was carried out with $ND_3$, and despite deuterium scrambling, the sites of H/D exchange at the time of fragmentation may not be identical to exchange with $CD_3OD$ because different exchange mechanisms are involved. The $y_7$ and $y_8$ ions are almost identical in the amount of deuterium retention. This is expected since the difference between the $y_7$ and $y_8$ ions is one proline residue, which has no labile hydrogens. On average, the $y_6$ ion retains

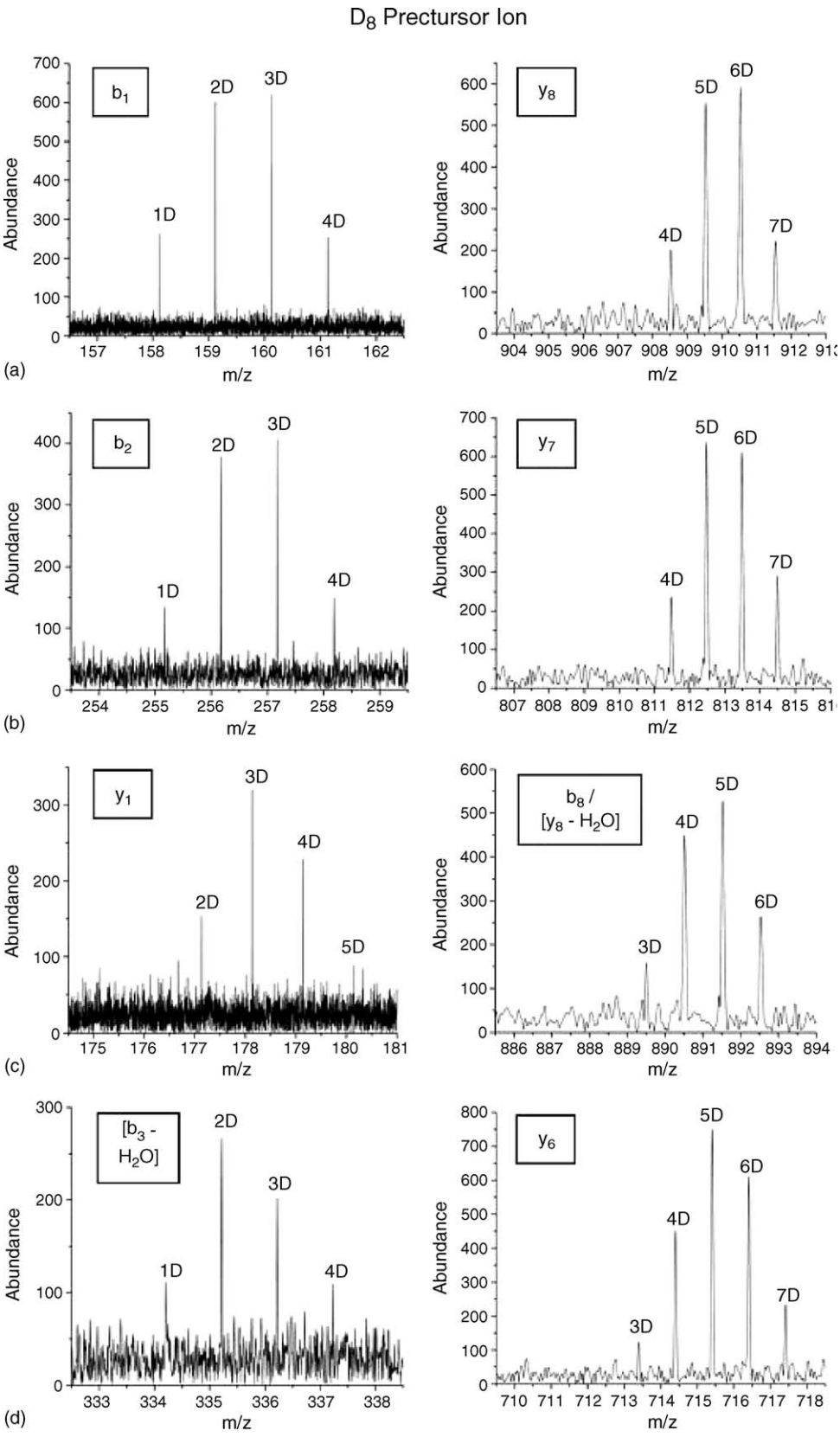


Fig. 5. Ion pairs and pseudo-ion pairs observed for the SORI-CID (SORI time = 500 ms, amplitude = 3 V) of the monoisotopically selected $D_8$ population (precursor ion monoisotopically selected before H/D exchange with $CD_3OD$ at $4 \times 10^{-7}$ Torr for 90 s): (a) $b_1$ and $y_8$; (b) $b_2$ and $y_7$; (c) $y_1$ and $b_8/[y_8 - H_2O]$ ($MS^3$ shows $b_8$ is major ion, see text); and (d) $[b3 - H_2O]$ and $y_6$.

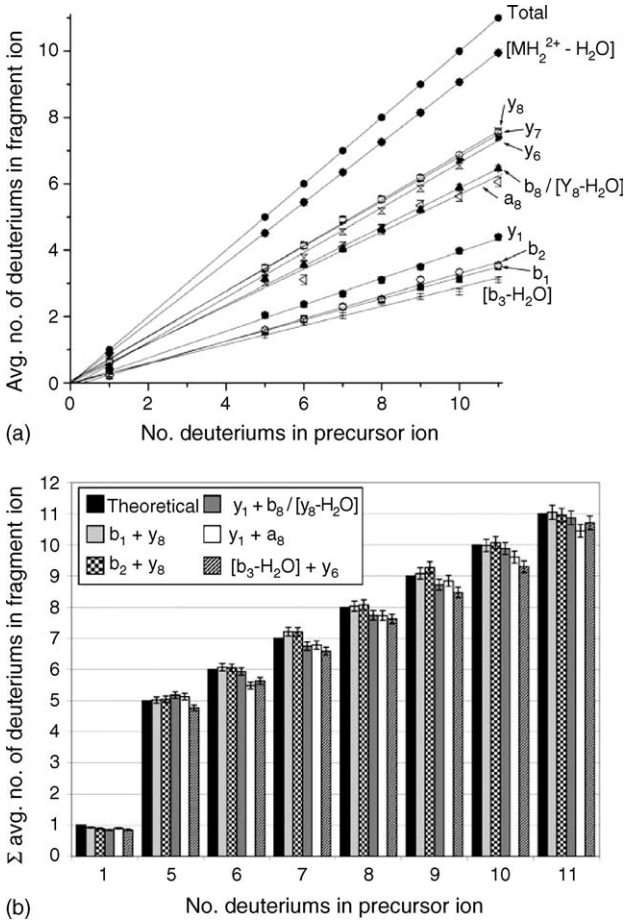


Fig. 6. Deuterium incorporation into fragment ions for the SORI-CID of $D_1$ and $D_5$–$D_{11}$ ion populations of doubly-protonated bradykinin after H/D exchange for 90 s with $CD_3OD$ at a pressure = $4 \times 10^{-7}$ Torr: (a) individual fragment ions with linear fit of data points and (b) sum of average deuterium incorporation for ion pairs and pseudo-ion pairs.

0.2 fewer deuteriums than the $y_7$ and $y_8$ ions over all populations studied. This is likely due to transfer of the exchanged hydrogen of the glycine amide to the newly formed $b_3$ ion. The $b_1$ and $b_2$ ions show an almost identical amount of retention of deuterium, as expected and discussed above for the $y_7$ and $y_8$ ions. Also, the $[b_3 - H_2O]$ ion retains the least amount of deuterium, indicating that some deuterium is lost with the neutral loss of water.

The $y_6$, $y_7$, and $y_8$ ions show greater retention of deuterium than the $a_8$ and $b_8$ (with some contribution from $[y_8 - H_2O]$) ions. Similarly, the $y_1$ ion retains more deuterium than the $b_1$ and $b_2$ ions. As noted in the previous section, this agrees with an earlier study which showed that y-type ions generally have more deuterium incorporated than b-type ions [24]. However, this does not agree with conclusions made in the same study that the first three exchanges are equivalent and occur at the protonated N-terminus, but the exchange reagent used in that study was $ND_3$ which may exchange directly with the terminal amino group [24]. As shown in Fig. 6a, fragmentation of the $D_5$ population results in average retention of less than two deuteriums by the $b_1$ and $b_2$ ions. Although scrambling could be occurring, the consistency with which the y-ions, including $y_1$, contain more deuterium than the corresponding b-ions, including $b_1$, suggests more facile exchange at the C-terminal arginine residue.

Fig. 6b shows the sum of the average number of deuteriums incorporated into the ion pairs $b_1/y_8$, $b_2/y_7$, and $y_1/b_8$ (with some $[y_8 - H_2O]$ contribution), and the pseudo-ion pairs $y_1/a_8$ and $[b_3 - H_2O]/y_6$. Excellent matches to theoretical for all ion populations are obtained for the ion pairs $b_1/y_8$ and $b_2/y_7$. This indicates these ions of a given complementary pair are likely being formed simultaneously through the same mechanism. The ion pair $y_1/b_8$ (with some $[y_8 - H_2O]$ contribution) also closely matches the theoretical for most ion populations despite having a mixed composition. It is likely that, although $y_8$ is expected to retain more deuterium, the excess deuterium is lost with the neutral water loss, causing $b_8$ and $[y_8 - H_2O]$ to retain very similar amounts of deuterium. A much poorer match to theoretical is found for the pseudo-ion pair $y_1/a_8$, with the sum of the deuterium incorporations consistently slightly lower than the theoretical for most ion populations. One of the mechanisms thought to occur for the formation of an $a_n$ ion is loss of CO from the $b_n$ ion [39–43]. However, this mechanism does not involve hydrogen. If this is the only mechanism occurring to form the $a_8$ ion, then the sum of the deuterium incorporation into the $y_1/a_8$ pseudo-ion pair is expected to match the theoretical value for each ion population (assuming $y_1$ and $b_8$ are formed by the same mechanism). Therefore, it is possible that the $a_8$ ion is being formed, at least some of the time, by another mechanism. Deuterium incorporation into the pseudo-ion pair $[b_3 - H_2O]/y_6$ is also lower than the theoretical value for all ion populations studied. However, this deviation may be due to some amount of deuterium being lost with the neutral water loss.

### 3.5. H/D exchange of $[RVYIFPF + 2H]^{2+}$

The seven amino acid residue peptide RVYIFPF is an analogue of angiotensin III (RVYIHPF) with the fifth residue replaced with phenylalanine. The doubly-protonated peptide, $[RVYIFPF + 2H]^{2+}$ has 15 labile hydrogens, including 1 carboxy terminus, 1 tyrosine, 2 amino terminal, 4 arginine and 5 backbone amide hydrogens, plus 2 ionizing protons. The FT-ICR monoisotopic isolation and H/D exchange with $CD_3OD$ of doubly-protonated RVYIFPF after 60, 360, and 600 s is shown in Fig. 7. After 60 s of exchange (Fig. 7a), two distinct ion populations with different rates of H/D exchange are evident. One population exchanges more slowly with $D_0$ as most abundant ion, while the second population exchanges more quickly with $D_7$ as the most abundant ion. The slower exchanging population accounts for approximately 90% of the overall ion abundance, in contrast to published data [7] for a modified peptide, $[t$TMP-$P^+$LDIFSDF + 1H$]^{2+}$, where the slower exchanging population accounts for only 10%. The maximum number of deuteriums incorporated into the precursor ion is 10. After 360 s of exposure to the $CD_3OD$ reagent at $1 \times 10^{-7}$ Torr (Fig. 7b), two additional exchanges are observed. Two distinct ion populations are still evident with $D_2$ and $D_8$ as the most abundant ions for the slower and faster exchanging populations, respectively. After 600 s of exchange, three distinct ion populations emerge, as indicated in Fig. 7c. These three ion populations have maximum abundance

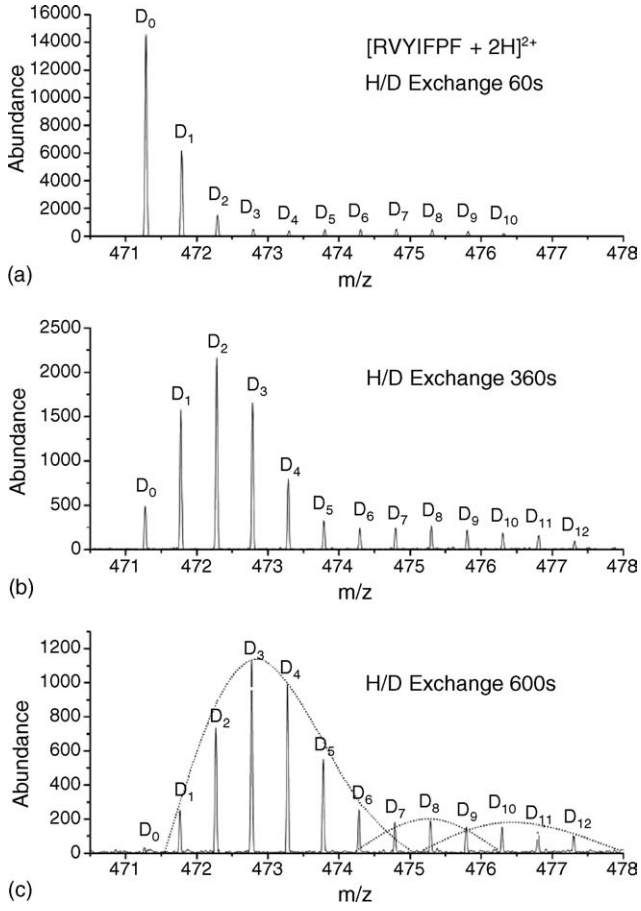


Fig. 7. Monoisotopic isolation and H/D exchange of $[RVYIFPF + 2H]^{2+}$ with $CD_3OD$ at $1 \times 10^{-7}$ Torr for: (a) 60 s, (b) 360 s and (c) 600 s. Peaks are labeled as $D_n$, where $n$ indicates the number of hydrogens which have been exchanged for deuterium.

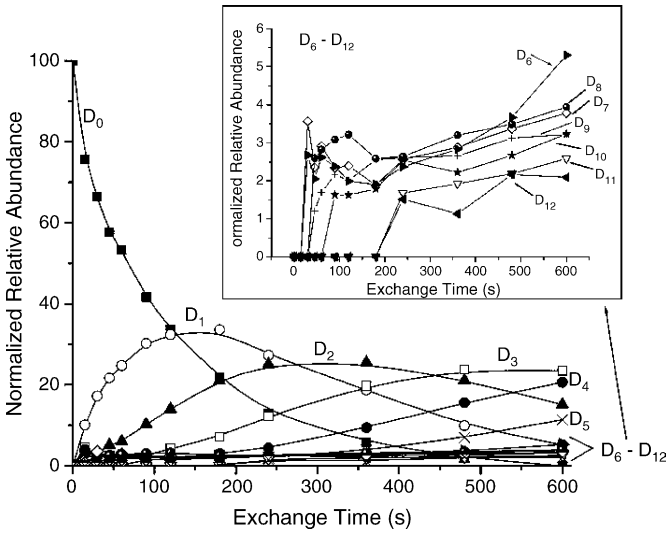


Fig. 8. Normalized relative abundance curves for deuterium incorporation into $[RVYIFPF + 2H]^{2+}$ after exposure to $CD_3OD$ at $1 \times 10^{-7}$ Torr from 0–600 s. Curves are labeled $D_n$, where $D_n$ indicates the number of hydrogens exchanged for deuterium. Inset shows expanded curves for $D_6$–$D_{12}$ (data points connected by straight lines in the inset).

ions at $D_3$, $D_8$, and $D_{10}$. The populations likely have different H/D exchange rates due to the spatial distribution of the atoms (i.e., conformation) and/or the location of the protons and hydrogen-bonding scheme. It is important to note that the distribution of deuterium in each population may become wider as a function of time. For example, $D_3$ in Fig. 6c (600 s exchange) likely corresponds to $D_0$ or $D_1$ in Fig. 6a (60 s exchange).

The normalized relative abundance curves for the incorporation of deuterium into $[RVYIFPF + 2H]^{2+}$ as a function of time for FT-ICR H/D exchange is shown in Fig. 8. The normalized relative abundance curves for $D_0$–$D_5$ account for the majority of the overall ion abundance over the exchange time studied. Furthermore, the slowest exchanging ion population is the main contributor to these curves (see Fig. 7). Apparent rate constants for the first four exchanges ($k_1$–$k_4$) are $8.0 \times 10^{-13}$, $5.7 \times 10^{-13}$, $4.9 \times 10^{-13}$, and $3.9 \times 10^{-13}$ mol s$^{-1}$ cm$^{-3}$. The normalized relative abundance curves for $D_6$–$D_{12}$ (Fig. 8, inset) show complicated kinetics due to contributions from at least three conformations/protonation motifs.

It is important to note that preliminary results for $[RVYIFPF + 2H]^{2+}$ H/D exchange with $D_2O$ for 10 s in a quadrupole ion trap indicated the existence of at least two distinct ion populations (data not shown). FT-ICR H/D exchange has advantages over QIT including the ability to track H/D exchange over a longer time period, which may lead to the observation of subtle exchange behavior (i.e., three populations shown in Fig. 7c). However, QIT H/D exchange is less expensive and more rapid (due to a higher reagent pressure). H/D exchange in an FT-ICR and in an ion trap can therefore be considered complementary methods.

### 3.6. Fragmentation of $[RVYIFPF + 2H]^{2+}$ ion populations labeled by H/D exchange

Following monoisotopic isolation and H/D exchange of the $[RVYIFPF + 2H]^{2+}$ precursor ion for 60 s at a $CD_3OD$ pressure of $1 \times 10^{-7}$ Torr, ion populations $D_1$–$D_7$ were monoisotopically selected and fragmented via SORI-CID over a range of SORI amplitudes. Fig. 9 shows representative data obtained for monoisotopic isolation and SORI-CID of the precursor ion with two and seven deuteriums incorporated ($D_2$ and $D_7$, respectively). Fig. 9a and b show the result of applying 1.0 and 1.5 V SORI pulses, respectively (SORI time = 500 ms, 500 ms argon pulse), to fragment the $D_2$ population. The insets in Fig. 9a and b show the isotopic distribution of the $y_2$ and $b_5$ fragment ions, where 0D, 1D, and 2D indicate zero, one, and two deuteriums, respectively. The singly-protonated $y_2$ and $b_5$ ions result from cleavage of the peptide bond between the fifth (phenylalanine) and sixth (proline) amino acid residues. The isotopic distribution of the $y_2$ and $b_5$ ions is similar in Fig. 9a and b, indicating the SORI amplitude over the range studied does not have an effect on the partitioning of the deuteriums. For the fragmentation of the $D_2$ ion population and over all SORI amplitudes studied, including the ones shown in Fig. 9a and b, the $y_2$ fragment ion contains zero or one deuterium, an average of 0.49, while the $b_5$ fragment ion contains two or one deuteriums, an average of 1.47. The sum of these average amounts of deuterium incorporation is

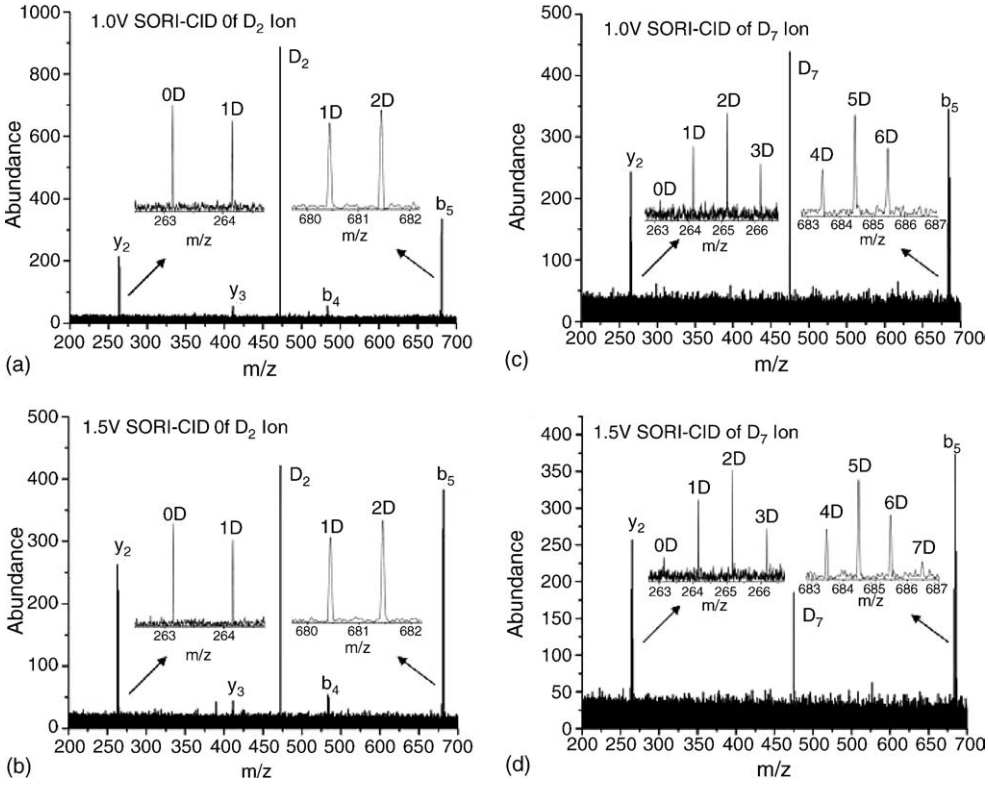


Fig. 9. Monoisotopic isolation and H/D exchange of $[RVYIFPF + 2H]^{2+}$ with $CD_3OD$ at $1 \times 10^{-7}$ Torr, followed by monoisotopic isolation of ion with two or seven deuteriums incorporated ($D_2$, *m/z* 472.3 or $D_7$, *m/z* 474.5) and SORI-CID with argon as the collision gas (500 ms pulse), SORI time = 500 m: (a) $D_2$, SORI amplitude = 1.0 V; (b) $D_2$, SORI amplitude = 1.5 V; (c) $D_7$, SORI amplitude = 1.0 V; and (d) $D_7$, SORI amplitude = 1.5 V. Insets show isotopic distribution of fragmentation ions with *n*D, indicating *n* number of deuteriums incorporated.

1.96, which agrees well with the theoretical value of 2 (two deuteriums incorporated in the precursor ion before SORI-CID). Similarly, Fig. 9c and d show the result of applying 1.0 and 1.5 V SORI pulses, respectively (SORI time = 500 ms, 500 ms argon pulse), to fragment the $D_7$ population. The partitioning of the deuterium atoms is not effected by SORI amplitude. For the fragmentation of the $D_7$ ion population and over all SORI amplitudes studied, including the ones shown in Fig. 9c and d, the $y_2$ fragment ion contains zero, one, two, or three deuteriums, an average of 1.93, while the $b_5$ fragment ion contains four, five, six, or seven deuteriums, an average of 5.16. The sum of the average deuterium incorporation is 7.09, which agrees well with the theoretical value of 7.0.

Fig. 10 shows the partitioning of the deuterium atoms in the $y_2$ and $b_5$ fragment ions for monoisotopic isolation and SORI-CID of $D_1$–$D_7$ $[RVYIFPF + 2H]^{2+}$ populations. Each data point represents the average amount of deuterium incorporated into the fragment ions averaged over a range of SORI amplitudes (i.e., 0, 0.5, 0.75, 1.0, 1.25, and 1.5 V SORI). Fragmentation is observed at 0 V SORI when collision gas is introduced due to heating that occurs upon monoisotropic isolation. SORI amplitude did not have any observable effect on the deuterium partitioning, as reflected in the error bars (standard deviation) in Fig. 10. The $y_2$ fragment ion can have a maximum of three deuteriums (i.e., one backbone amide, one carboxy terminus, and one ionizing deuterium). As illustrated in Fig. 10, the $y_2$ fragment ion has an average of two deuteriums incorporated when the precursor ion is labeled with seven deuteriums. The corresponding $b_5$ fragment ion can have a maximum of 12 deuteriums incorporated (i.e., 1 ionizing, 1 tyrosine, 2 amino terminal, 4 backbone amide, and 4 arginine deuteriums). When the precursor ion is labeled

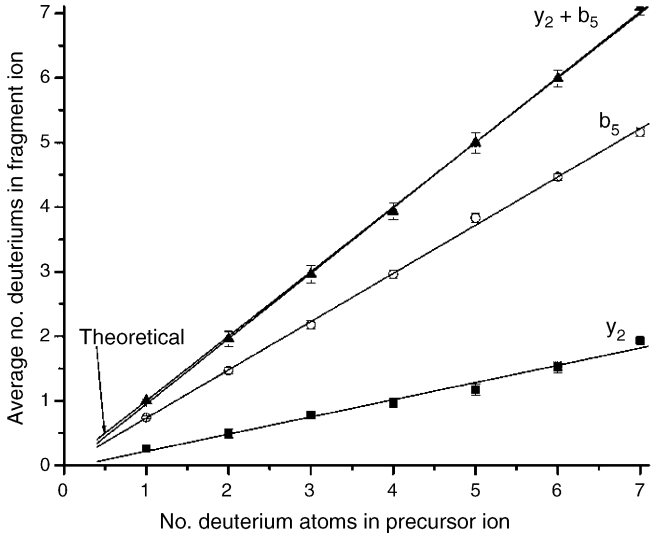


Fig. 10. Partitioning of deuterium atoms in the $y_2$ and $b_5$ fragment ions for the SORI-CID (SORI time = 500 ms, argon pulse = 500 ms) of $[RVYIFPF + 2H]^{2+}$ with one to seven deuteriums incorporated ($D_1$–$D_7$). Data points represent the average number of deuteriums incorporated into the indicated fragment ion for SORI amplitude = 0, 0.5, 0.75, 1.0, 1.25, and 1.5 V.

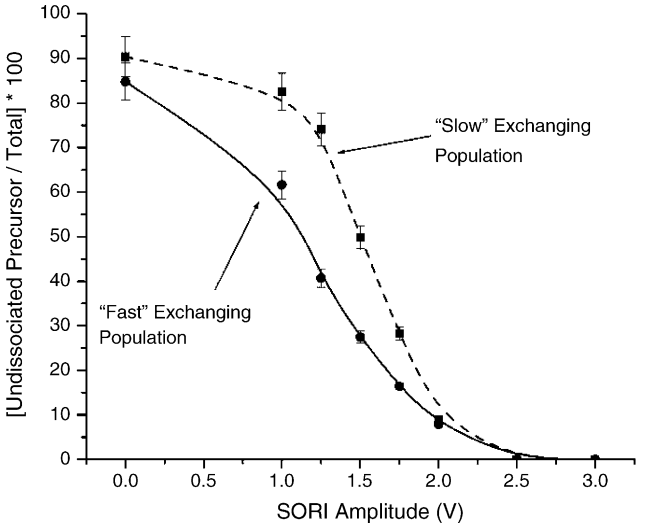


Fig. 11. Precursor survival yield for slower- and faster-exchanging $[RVYIFPF + 2H]^{2+}$ populations (H/D exchange with $CD_3OD$ at $1 \times 10^{-6}$ Torr for 60 s) as a function of SORI amplitude (SORI time = 500 ms).

with seven deuteriums, the $b_5$ fragment ion has an average of five deuteriums incorporated (Fig. 10). The sum of the average number of deuterium atoms incorporated into the $y_2$ and $b_5$ ions matches very closely with the theoretical, as shown in Fig. 10. This indicates that the $y_2/b_5$ ion pair is complementary, consistent with conclusions for the $y_2/b_5$ ions of doubly-protonated angiotensin II (DRVYIHPF) using kinetic energy release distributions (KERDs) [45]. While scrambling of the deuterium atoms before or during the fragmentation event cannot be ruled-out, the partitioning of the deuterium atoms demonstrates that both fragment ions are being formed by the same mechanism.

While the partitioning of the deuterium atoms is not affected by SORI amplitude over the range studied (i.e., 0.5–1.5 V SORI, as discussed above), SORI amplitude does effect extent of fragmentation for the different ion populations. Fig. 11 shows the precursor ion survival yield as a function of SORI amplitude for the "slower" and "faster" exchanging $[RVYIFPF + 2H]^{2+}$ ion populations. In this experiment, the exchange was carried out for 60 s, but at a $CD_3OD$ pressure an order of magnitude greater ($1 \times 10^{-6}$ Torr) than was used to generate the data in Fig. 7. Therefore, the distribution of deuterium atoms after 60 s of exchange at $1 \times 10^{-6}$ Torr was similar to that shown in Fig. 7b (H/D exchange for 360 s at $1 \times 10^{-7}$ Torr). Following H/D exchange, the envelopes of peaks corresponding to $D_0$–$D_5$ and $D_6$–$D_{12}$, and therefore the "slower" and "faster" exchanging populations, respectively, were isolated and fragmented over a range of SORI amplitudes (0–3 V). As shown in Fig. 11, the "fast" exchanging population displays a higher extent of fragmentation at lower SORI amplitudes than does the "slow" exchanging population. Presumably, the different ion populations have different H/D exchange behaviors due to different conformations/protonation motifs, and the different conformations/protonation motifs are also affecting the SORI amplitude required to observe the same level of fragmentation. Upon activation, the ion populations may convert into distinct "energized" structures, as illustrated in Scheme 1b, and these distinct "energized" structures have different fragmentation efficiencies. As discussed above for doubly-protonated bradykinin, the difference in fragmentation efficiencies may also be due to a difference in collisional cross-section, and therefore a difference in the number of collisions in a given SORI activation time. The observed differences in activation energy requirements cannot be contributed to a deuterium isotope effect, which would cause ion populations labeled with more deuterium ions to have lesser levels of fragmentation at greater SORI amplitudes.

## 4. Conclusions

Gas phase H/D exchange can be a selective technique to separate different non-interconverting isomers, even when these conformations, likely with different hydrogen bonding motifs, are not distinguishable by standard ion mobility techniques. Furthermore, these different ion populations may have different fragmentation efficiencies, as demonstrated for the doubly-protonated peptides bradykinin and RVYIFPF, an angiotensin III analogue. The observed differences are not due to a deuterium isotope effect, as demonstrated by back-exchange and fragmentation of doubly-protonated bradykinin. These results clearly demonstrate that conformation/protonation motif plays an important role in the unimolecular dissociation of peptide ions. The overall fragmentation characteristics observed for a protonated peptide are therefore an average of the fragmentation characteristics of individual ion populations with different conformation/protonation motifs.

Deuterium incorporation in $b_n/y_{m-n}$ ion pairs can provide evidence that the ions are being formed during the same fragmentation event if the sum of the average deuterium incorporation into the $b_n$ and $y_{m-n}$ ions matches the overall amount of deuterium in the precursor ion. This partitioning of deuterium atoms will match the theoretical value regardless of whether deuterium scrambling is occurring before or during the fragmentation event because the complementary ions are formed via one mechanism. An FT-ICR is appropriate for this type of study because of multiple analysis steps including monoisotopic selection of the precursor ion, H/D exchange with excellent time and pressure control, and monoisotopic selection and SORI-CID of individual ion populations. The overall deuterium incorporation into the $b_1/y_8$ and $b_2/y_7$ bradykinin ion pairs and the $y_2/b_5$ RVYIFPF ion pair suggests these complementary ions are being formed by the same mechanism for the doubly-protonated precursor ions. Results for deuterium incorporation into the $y_1/a_8$ bradykinin pseudo-ion pair are consistently less than the theoretical values, suggesting some other mechanism for the $a_8$ ion formation may be involved, or that the $y_1/b_8$ ions form by multiple mechanisms.

## Acknowledgement

This research was supported by the National Institutes of Health grant 2 R01 GM051387 to V.H. Wysocki.

## References


[1] F. Wang, M.A. Freitas, A.G. Marshall, B.D. Sykes, Int. J. Mass Spectrom. 192 (1999) 319.
[2] C.S. Hoaglund-Hyzer, A.E. Counterman, D.E. Clemmer, Chem. Rev. 99 (1999) 3037.
[3] M.F. Jarrold, Acc. Chem. Res. 32 (1999) 360.
[4] W.D. Price, R.A. Jockusch, E.R. Williams, J. Am. Chem. Soc. 120 (1998) 3474.
[5] C.J. Cassady, S.R. Carr, J. Mass Spectrom. 31 (1996) 247.
[6] A.R. Dongre, J.L. Jones, A. Somogyi, V.H. Wysocki, J. Am. Chem. Soc. 118 (1996) 8365.
[7] K.A. Herrmann, V.H. Wysocki, E.R. Vorpagel, J. Am. Soc. Mass Spectrom. 16 (2005) 1067.
[8] D. Suckau, Y. Shi, S.C. Beu, M.W. Senko, J.P. Quinn, F.M. Wampler, F.W. McLafferty, Proc. Natl. Acad. Sci. U.S.A. 90 (1993) 790.
[9] F.W. McLafferty, Z.Q. Guan, U. Haupts, T.D. Wood, N.L. Kelleher, J. Am. Chem. Soc. 120 (1998) 4732.
[10] M.A. Freitas, C.L. Hendrickson, M.R. Emmett, A.G. Marshall, J. Am. Soc. Mass Spectrom. 9 (1998) 1012.
[11] T. Wyttenbach, M.T. Bowers, Modern Mass Spectrometry, vol. 225, 2003, p. 207.
[12] M.K. Green, C.B. Lebrilla, Int. J. Mass Spectrom. 175 (1998) 15.
[13] S. Campbell, M.T. Rodgers, E.M. Marzluff, J.L. Beauchamp, J. Am. Chem. Soc. 117 (1995) 12840.
[14] E. Gard, M.K. Green, J. Bregar, C.B. Lebrilla, J. Am. Soc. Mass Spectrom. 5 (1994) 623.
[15] A.C. Gill, K.R. Jennings, T. Wyttenbach, M.T. Bowers, Int. J. Mass Spectrom. 196 (2000) 685.
[16] T. Wyttenbach, G. vonHelden, M.T. Bowers, J. Am. Chem. Soc. 118 (1996) 8355.
[17] A.E. Counterman, S.J. Valentine, C.A. Srebalus, S.C. Henderson, C.S. Hoaglund, D.E. Clemmer, J. Am. Soc. Mass Spectrom. 9 (1998) 743.
[18] B.M. Moscato, E.M. Marzluff, Abstr. Pap. Am. Chem. Soc. 229 (2005) U454.
[19] H.A. Sawyer, J.T. Marini, E.G. Stone, B.T. Ruotolo, K.J. Gillig, D.H. Russell, J. Am. Soc. Mass Spectrom. 16 (2005) 893.
[20] C. Lifshitz, Int. J. Mass Spectrom. 234 (2004) 63.
[21] B.G. Reuben, Y. Ritov, O. Geller, M.A. McFarland, A.G. Marshall, C. Lifshitz, Chem. Phys. Lett. 380 (2003) 88.
[22] D.M. Mao, D.J. Douglas, J. Am. Soc. Mass Spectrom. 14 (2003) 85.
[23] R.W. Purves, D.A. Barnett, B. Ells, R. Guevremont, Rapid Commun. Mass Spectrom. 15 (2001) 1453.
[24] E. Levy-Seri, G. Koster, A. Kogan, K. Gutman, B.G. Reuben, C. Lifshitz, J. Phys. Chem. A 105 (2001) 5552.
[25] T.G. Schaaff, J.L. Stephenson, S.A. McLuckey, J. Am. Soc. Mass Spectrom. 11 (2000) 167.
[26] T.G. Schaaff, J.L. Stephenson, S.A. McLuckey, J. Am. Chem. Soc. 121 (1999) 8907.
[27] M.A. Freitas, A.G. Marshall, Int. J. Mass Spectrom. 183 (1999) 221.
[28] T. Wyttenbach, M.T. Bowers, J. Am. Soc. Mass Spectrom. 10 (1999) 9.
[29] P.D. Schnier, W.D. Price, R.A. Jockusch, E.R. Williams, J. Am. Chem. Soc. 118 (1996) 7178.
[30] K. Biemann, Biomed. Environ. Mass Spectrom. 16 (1988) 99.
[31] C.W. Tsang, A.G. Harrison, J. Am. Chem. Soc. 98 (1976) 1301.
[32] D.R. Mueller, M. Eckersley, W.J. Richter, Org. Mass Spectrom. 23 (1988) 217.
[33] R.S. Johnson, D. Krylov, K.A. Walsh, J. Mass Spectrom. 30 (1995) 386.
[34] A.G. Harrison, T. Yalcin, Int. J. Mass Spectrom. 165 (1997) 339.
[35] C.G. Gu, G. Tsaprailis, L. Breci, V.H. Wysocki, Anal. Chem. 72 (2000) 5804.
[36] C.Q. Jiao, D.R.A. Ranatunga, W.E. Vaughn, B.S. Freiser, J. Am. Soc. Mass Spectrom. 7 (1996) 118.
[37] J.E. Bartmess, R.M. Georgiadis, Vacuum 33 (1983) 149.
[38] S. Gronert, J. Am. Soc. Mass Spectrom. 9 (1998) 845.
[39] B. Paizs, Z. Szlavik, G. Lendvay, K. Vekey, S. Suhai, Rapid Commun. Mass Spectrom. 14 (2000) 746.
[40] K. Ambihapathy, T. Yalcin, H.W. Leung, A.G. Harrison, J. Mass Spectrom. 32 (1997) 209.
[41] J.M. Farrugia, R.A.J. O'Hair, G.E. Reid, Int. J. Mass Spectrom. 210 (2001) 71.
[42] T. Yalcin, C. Khouw, I.G. Csizmadia, M.R. Peterson, A.G. Harrison, J. Am. Soc. Mass Spectrom. 6 (1995) 1165.
[43] T. Yalcin, I.G. Csizmadia, M.R. Peterson, A.G. Harrison, J. Am. Soc. Mass Spectrom. 7 (1996) 233.
[44] K.D. Ballard, S.J. Gaskell, J. Am. Soc. Mass Spectrom. 4 (1993) 477.
[45] J. Adams, F.H. Strobel, A. Reiter, M.C. Sullards, J. Am. Soc. Mass Spectrom. 7 (1996) 30.